

Electronic supplementary information for

Highly active hydrogen evolution electrocatalyst based on novel cobalt-nickel sulfide composite electrode†

Davide Ansovini,^{a,b} Coryl Jing Jun Lee,^a Chin Sheng Chua,^a Lay Ting Ong,^a Hui Ru Tan,^a William Webb,^b Robert Raja^b and Yee-Fun Lim^{*a}

^a Institute of Materials Research and Engineering (IMRE), A*STAR (Agency for Science, Technology and Research), 2 Fusionopolis Way, Innovis, #08-03, Singapore 138634, Republic of Singapore.

^b School of Chemistry, University of Southampton, Highfield, Southampton SO17 1BJ, United Kingdom.

*Email: limyf@imre.a-star.edu.sg

Experimental details

I. Materials synthesis

Cobalt nitrate hexahydrate ($\text{Co}(\text{NO}_3)_2 \cdot 6\text{H}_2\text{O}$, ACS reagent $\geq 98\%$), thiourea ($\text{CS}(\text{NH}_2)_2$, ACS reagent $\geq 99\%$), methanol (CH_3OH , anhydrous 99.8%), sulphuric acid (H_2SO_4), potassium hydroxide (KOH) were purchased from Sigma Aldrich, Fisher Scientific and used without further purification. Nickel foam ($\text{Ni} \geq 99.8\%$, PPI = 110, thickness = 1 mm, volumetric porosity $\geq 95\%$, area mass density = 300 g/m^2) was purchased from Latech Scientific Supply.

Synthesis of cobalt-thiourea complex ($\text{Co}(\text{CH}_4\text{N}_2\text{S})_4(\text{NO}_3)_2$)

The procedure was taken and adapted from Kumar *et al.*¹ For a typical synthesis, cobalt nitrate hexahydrate (2.3282 g, 0.008 mol) was dissolved in 20 mL of methanol under stirring at room temperature. The concentration of the cobalt ions was fixed at 0.4 M. Upon complete dissolution of the metal salt thiourea (2.4358 g, 0.032 mol) was added into the solution under stirring at room temperature. The molar ratio between thiourea and the cobalt salt was equal to 4. After thiourea was dissolved in the stirring solution the colour changed from dark pink to dark blue. The obtained complex was stirred for further 2 hours before being used for the next synthetic step.

Synthesis of Co_9S_8 - Ni_xS_y /Ni foam electrode

Ni foam (2 cm x 1.5 cm) was first ultrasonicated at room temperature in 1) 37% HCl_{aq} , 2) ethanol, 3) DI water, 4) acetone, each step for 5 minutes. At the end it was dried using a N_2 gun before further processing. All the synthetic steps were performed inside a N_2 -filled glovebox. Etched Ni foam (2cm x 1.5 cm) was dipped into the methanolic solution containing the fresh cobalt-thiourea complex for 1 min. Then the excess trapped solution in the pores was removed with a cotton cloth by capillarity. The foam was dried at 100°C for 2 minutes before being annealed at 300°C for 5 minutes. During this step the colour of the foam changed from pale silvery to black, with formation of visible vapours due to the thermal decomposition of the cobalt-thiourea complex. This cycle can be repeated in order to increase the metal loading. After the last cycle the

electrode was annealed at a selected temperature and time (400°C-500°C, 10 min-90 min). The electrode was then soldered to a Ni wire and the upper edge was sealed using silicone, defining a geometric area of 1 cm².

Synthesis of Ni₃S₂/Ni foam electrode

Thiourea (1.8269 g, 0.024 mol) was first dissolved in 20 mL of 2-methoxyethanol at room temperature. The molar concentration of thiourea was the same as for the Co-thiourea precursor and equal to 1.6 M. The procedure for the fabrication of the electrode is the same as that reported above.

II. Structural characterization

The electrodes were characterized by X-ray diffraction (XRD), scanning electron microscopy (SEM), transmission electron microscopy (TEM), Raman spectroscopy, energy-dispersive X-ray spectroscopy (EDX) and X-ray photoelectron spectroscopy (XPS). XRD patterns were acquired with a Rigaku SmartLab, using monochromatic Cu K α radiation (1.540598 Å). The morphology of the samples was characterized using a JEOL-JSM 7200 field-emission scanning electron microscope (FE-SEM) using an acceleration voltage of 15kV. EDX analysis for the determination of the elemental composition was carried out with the same SEM apparatus used for the morphological analysis. TEM and selected area electron diffraction (SAED) pattern imaging were carried out using Philips CM300 FEG TEM operated at an accelerating voltage of 300 kV. Raman measurements were performed using a Witec Alpha 300R confocal Raman microscope equipped with a 532 nm Nd:YAG laser. XPS data were collected with a Thermo Fisher Scientific Theta Probe X-ray photoelectron spectrometer using monochromatic Al K α radiation (1486.6 eV) as X-ray source. The binding energies were charge corrected using adventitious C 1s peak at 285.0 eV as reference.

III. Electrochemical characterization

All the electrochemical measurements were performed in a 3-electrode configuration using silver/silver chloride (Ag/AgCl (3 M KCl)) as reference, a Pt foil as counter and the sample as working electrode. The geometric area of the working electrode was set equal to 1 cm² for all the experiments. Linear sweep voltammetry (LSV) tests were carried out using a Metrohm Autolab PGSTAT101 potentiostat in 350 mL 1 M KOH (aq). Fresh deionized water (18 M Ω ·cm) was used for the preparation of the electrolyte. Before each experiment, the solution was purged for 30 minutes with pure argon in order to strip off any dissolved gas. The pH of the electrolyte was measured using a Fisher Scientific Accumet basic AB15 pH meter resulting equal 13.79. All the potentials were reported versus the reversible hydrogen electrode (RHE) using the following relation: $E_{\text{RHE}} = E_{\text{Ag/AgCl,3MKCl}}^0 + E_{\text{Ag/AgCl,3MKCl}} + 0.059 \cdot \text{pH}$, where $E_{\text{Ag/AgCl,3MKCl}}^0 = +0.210$ V vs RHE. For the LSV measurements the potential was scanned from 0 to -0.4 V versus RHE at a scan rate of 1 mV s⁻¹. For each sample, at least 20 LSV scans were performed, with the last scan always used for analysis. The polarization curves were iR-corrected for each sample. Electrochemical impedance spectroscopy (EIS) was carried out using a Metrohm Autolab PGSTAT302N potentiostat in potentiostatic mode at -0.230 V vs RHE, with a scanning frequency from 100 kHz to 50 mHz and an amplitude of 10 mV. The stability test was performed under chronoamperometric conditions at -0.161 V vs RHE (after iR correction) for 72 hours. Each data point of the measured current was taken every 5 seconds and the electrolyte was constantly stirred throughout the experiment in order to get rid of the hydrogen bubbles.

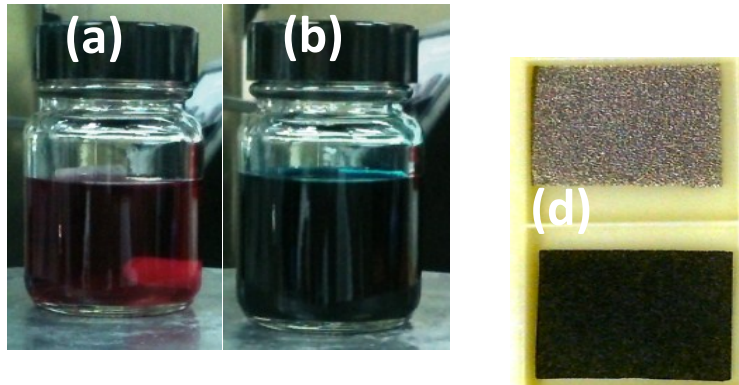


Fig. S1 (a) Cobalt nitrate dissolved in methanol before addition of thiourea, (b) after addition of thiourea; (c) bare Ni foam, (d) as synthesized $\text{Co}_9\text{S}_8\text{-Ni}_x\text{S}_y/\text{Nif}$ electrode.

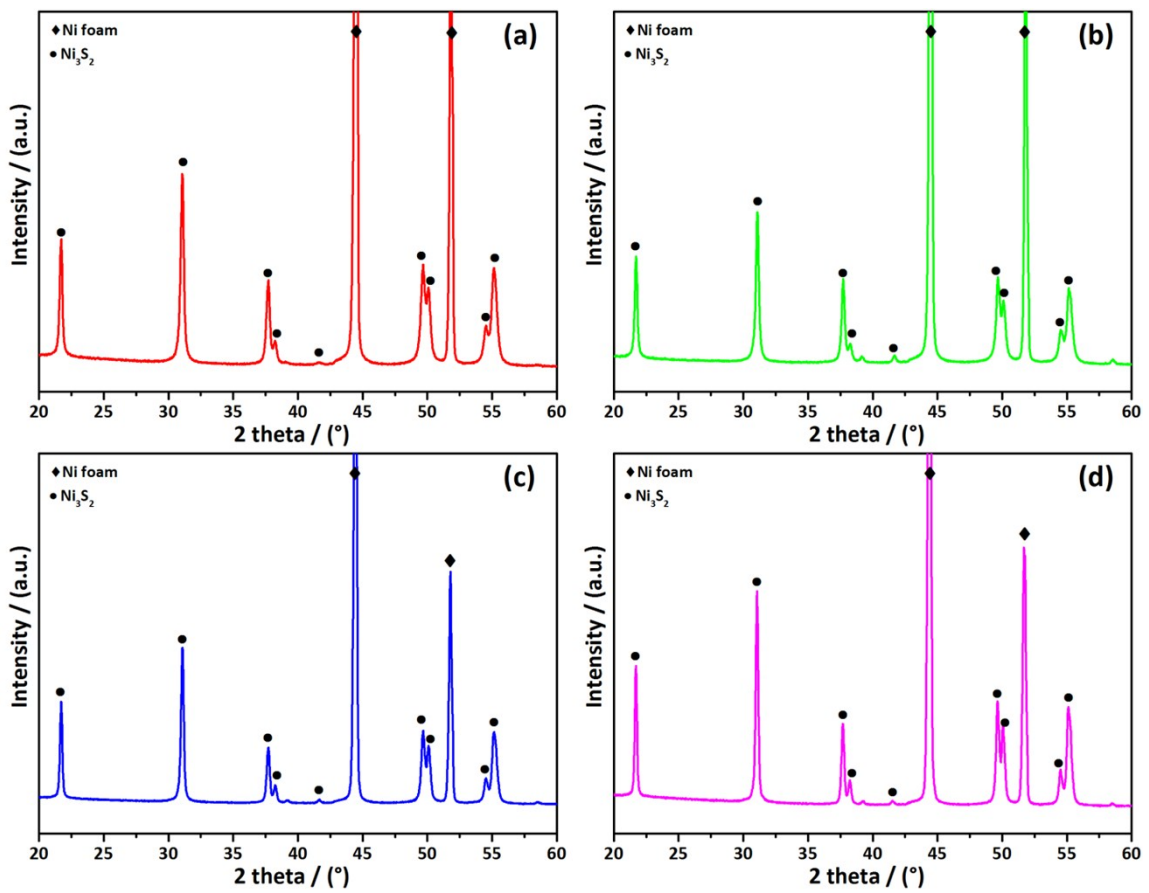


Fig. S2 XRD patterns for the $\text{Ni}_3\text{S}_2/\text{Nif}$ at different annealing temperatures and times (a) 400 °C 10 min, (b) 400°C 90 min, (c) 500°C 10 min, (d) 500°C 90 min.

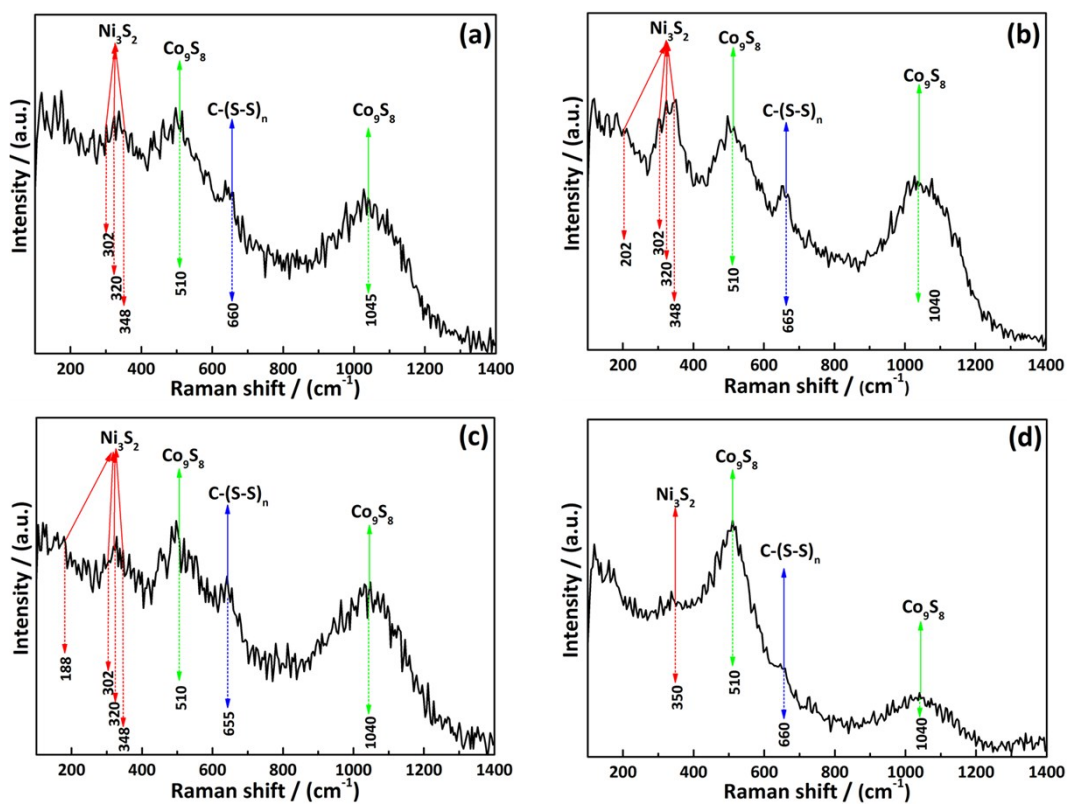


Fig. S3 Raman spectra for $\text{Co}_9\text{S}_8\text{-Ni}_x\text{S}_y/\text{Nif}$ at different annealing temperatures and times (a) 400 °C 10 min, (b) 400 °C 90 min, (c) 500 °C 10 min, (d) 500 °C 90 min.

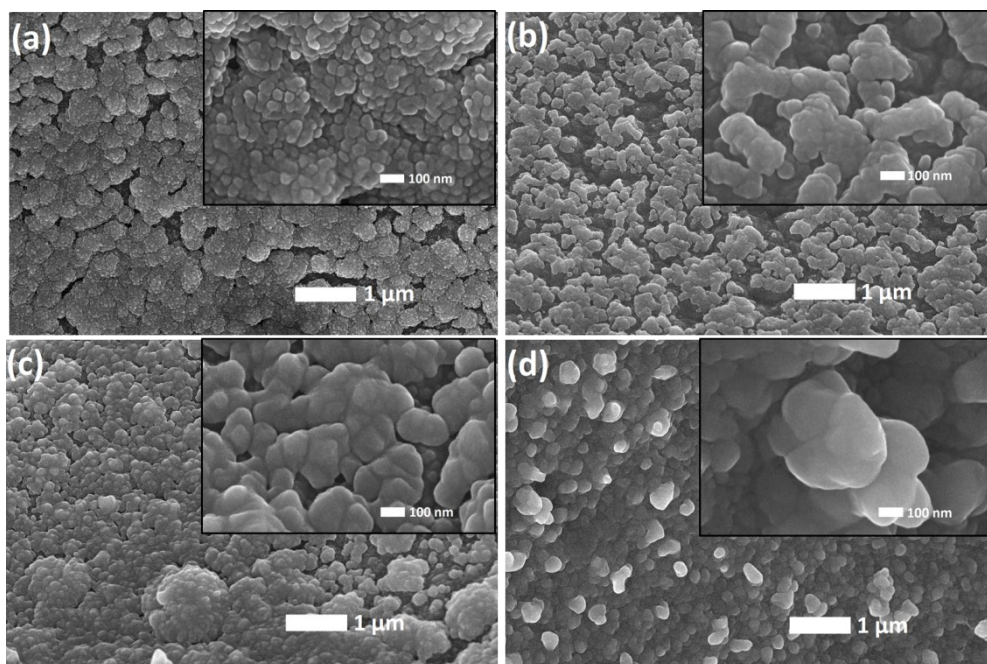


Fig. S4 Low- and high-magnification SEM images for $\text{Ni}_3\text{S}_2/\text{Nif}$ at different annealing temperatures and times (a) 400 °C 10 min, (b) 400 °C 90 min, (c) 500 °C 10 min, (d) 500 °C 90 min.

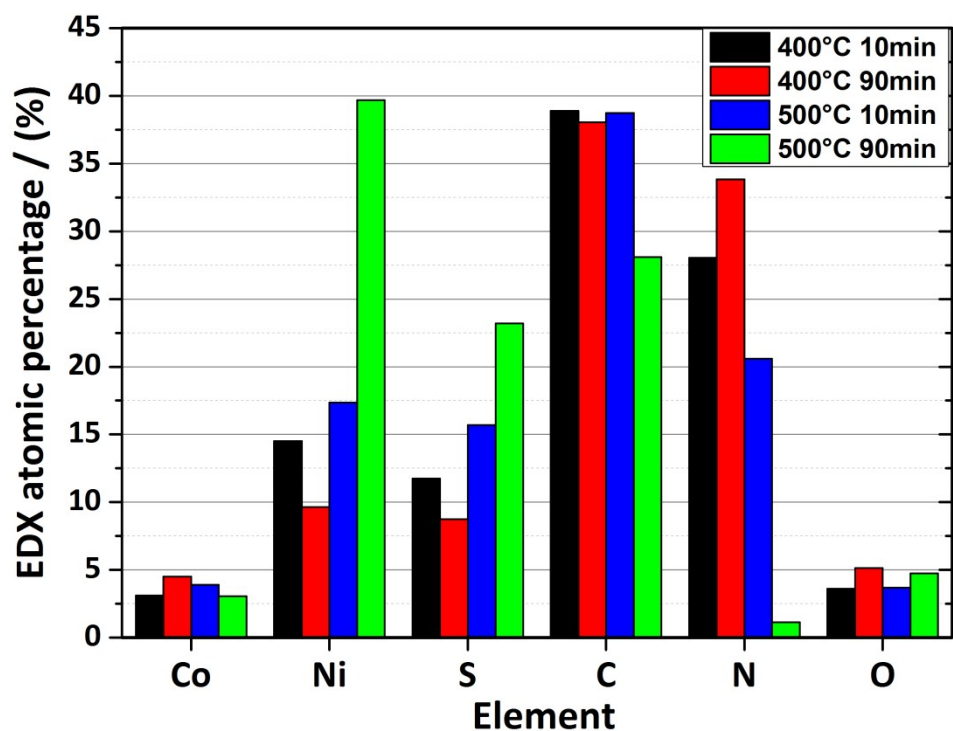


Fig. S5 EDX analysis for $\text{Co}_9\text{S}_8\text{-Ni}_x\text{S}_y/\text{Nif}$ at different annealing temperatures and times.

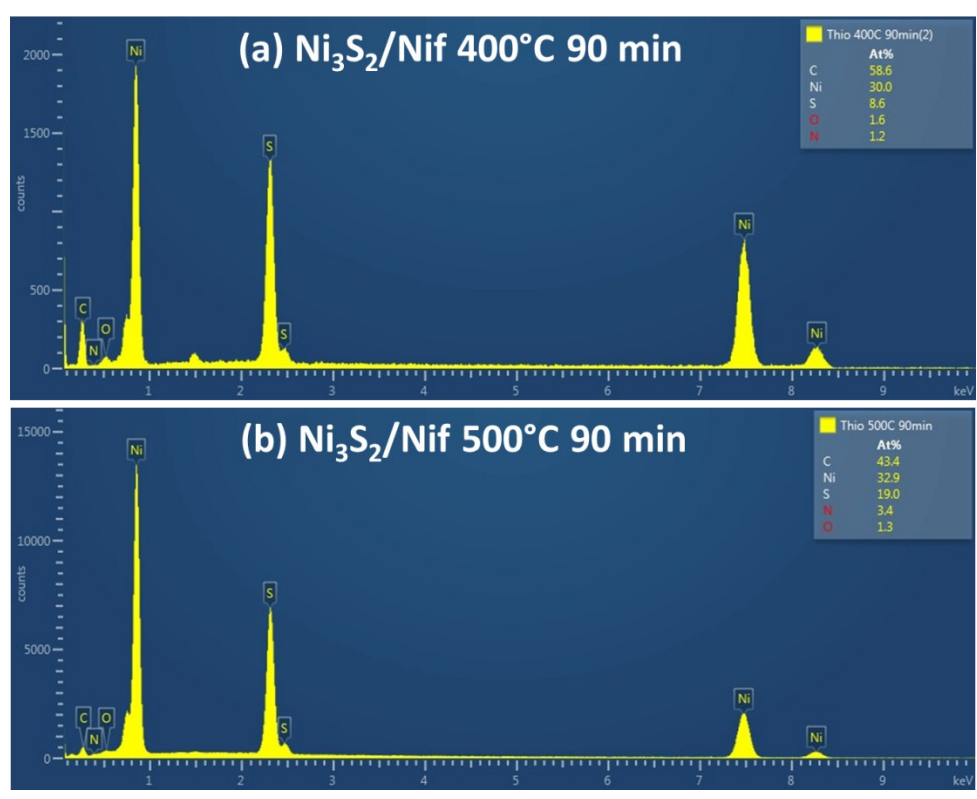


Fig. S6 EDX analysis for $\text{Ni}_3\text{S}_2/\text{Nif}$ at (a) 400 °C 90 min, (b) 500 °C 90 min.

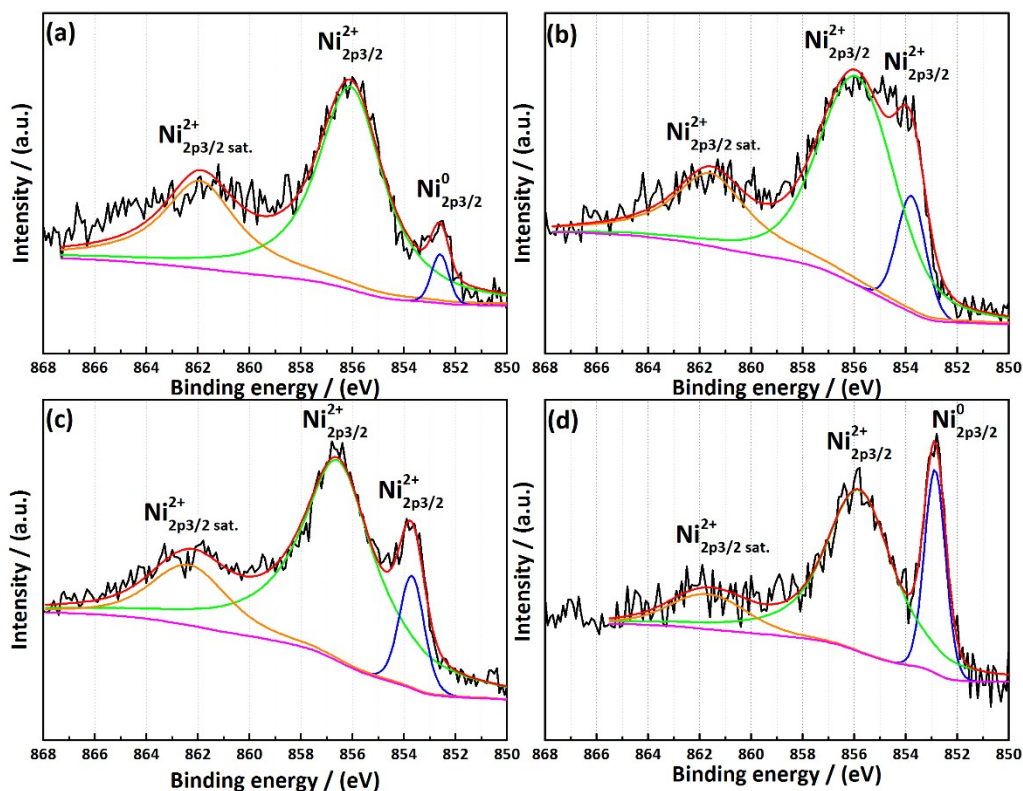


Fig. S7 Ni2p XPS patterns for $\text{Co}_9\text{S}_8\text{-Ni}_x\text{S}_y/\text{Nif}$ at different annealing temperatures and times (a) 400 °C 10 min, (b) 400°C 90 min, (c) 500°C 10 min, (d) 500°C 90 min.

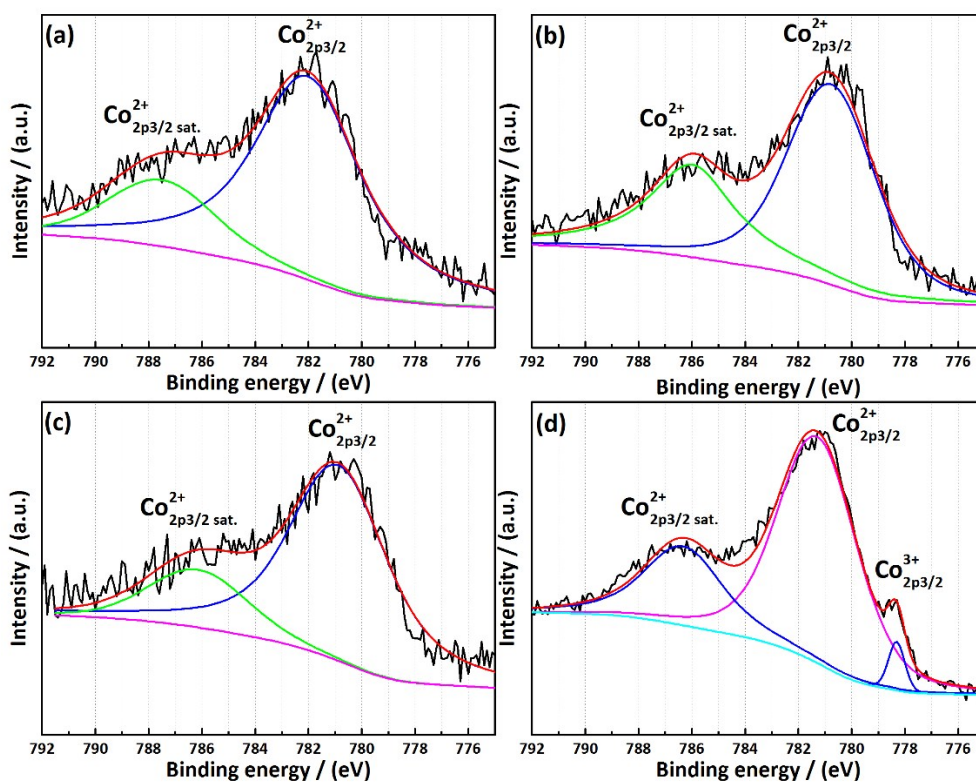


Fig. S8 Co2p XPS patterns for $\text{Co}_9\text{S}_8\text{-Ni}_x\text{S}_y/\text{Nif}$ at different annealing temperatures and times (a) 400 °C 10 min, (b) 400°C 90 min, (c) 500°C 10 min, (d) 500°C 90 min.

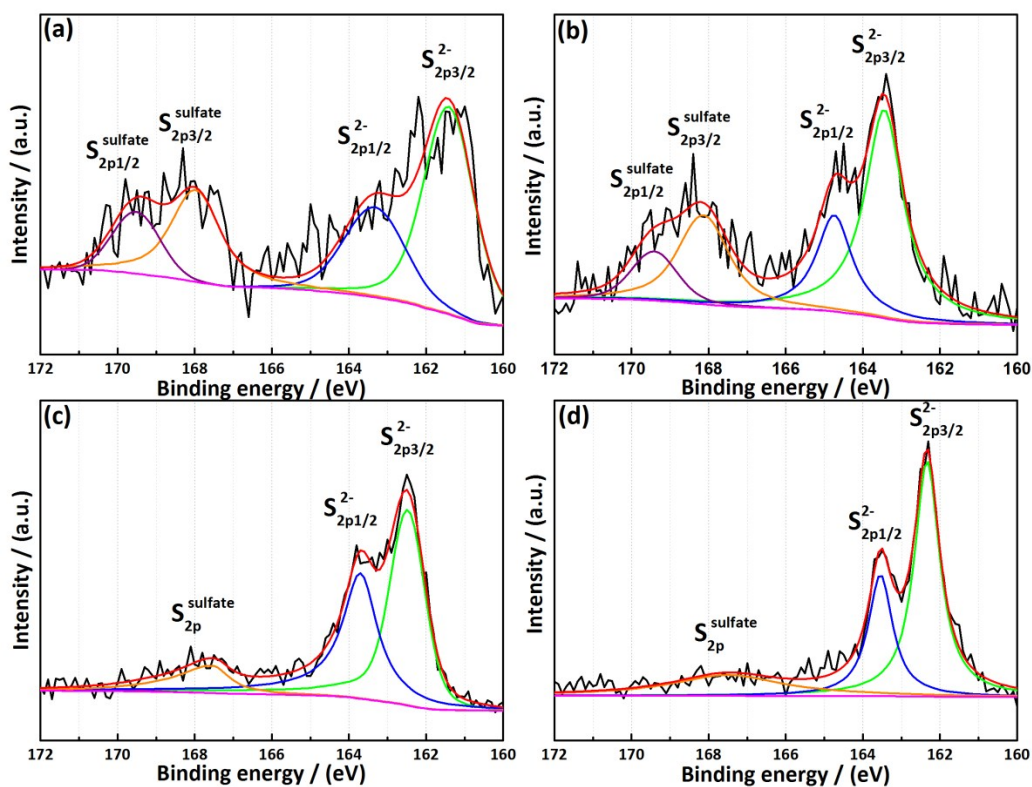


Fig. S9 S2p XPS patterns for $\text{Co}_9\text{S}_8\text{-Ni}_x\text{S}_y/\text{Nif}$ at different annealing temperatures and times (a) 400 °C 10 min, (b) 400 °C 90 min, (c) 500 °C 10 min, (d) 500 °C 90 min.

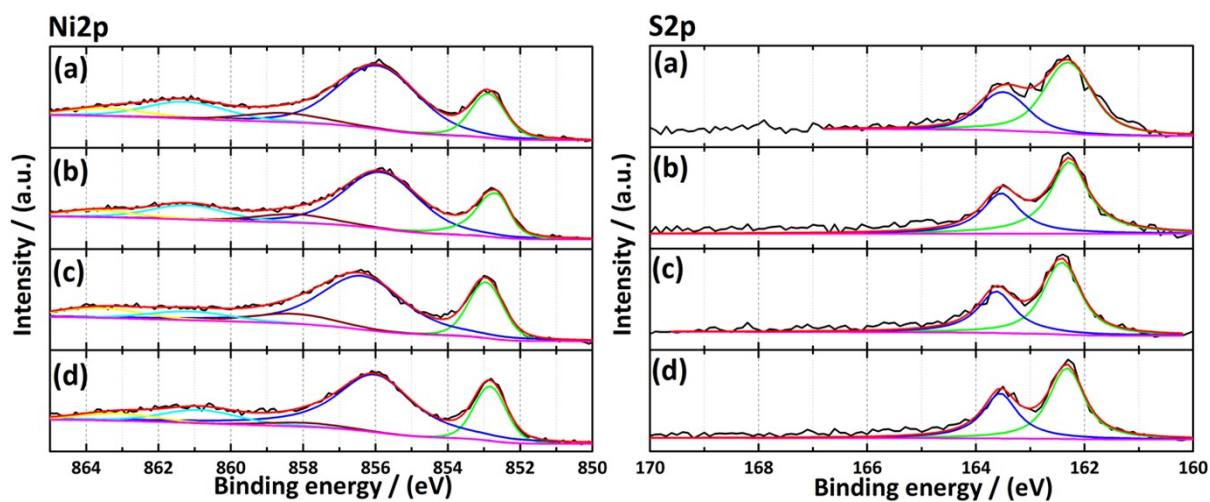


Fig. S10 Ni2p (left) and S2p (right) XPS patterns for $\text{Ni}_3\text{S}_2/\text{Nif}$ at different annealing temperatures and times (a) 400 °C 10 min, (b) 400 °C 90 min, (c) 500 °C 10 min, (d) 500 °C 90 min.

Annealing condition	Co/Ni atomic ratio	S/(Co+Ni) atomic ratio	Co ³⁺ /Co ²⁺ atomic ratio	S ²⁻ /(SO ₄ ²⁻) atomic ratio
400°C 10 min	1.22	1.02	0	1.95
400°C 90 min	1.04	0.99	0	2.0
500°C 10 min	0.53	0.74	0	6.37
500°C 90 min	3.28	0.68	0.04	29.85

Table S1 XPS quantitative analysis of the elemental composition on the surface of Co₉S₈-Ni_xS_y/Nif electrode for different synthetic conditions

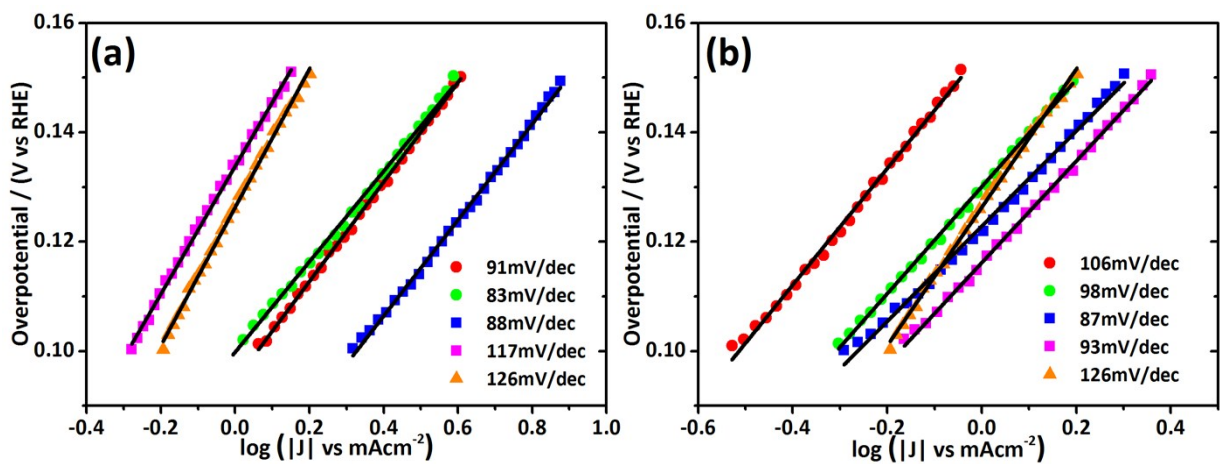


Fig. S11 iR-corrected Tafel plots for (a) Co₉S₈-Ni_xS_y/Nif and (b) Ni₃S₂/Nif at different annealing temperatures and times in 1M KOH electrolyte.

Material	Electrolyte	$\eta_{(10\text{mAcm}^{-2})}$	Tafel slope (mV/dec)	Reference
CoS ₂ nanopyramids/3D CFP	1M KOH	250	-	2
CoS ₂	1M KOH	244	133	3
Co ₉ S ₈ nanosheets	1M KOH	152	-	4
Co ₉ S ₈ /C	1M KOH	250	-	5
Zn _{0.76} Co _{0.24} S/CoS ₂	1M KOH	238 (20 mA/cm ²)	164	6
Amorphous CoSe	1M KOH	121	84	7
NiS ₂ nanosheets/CC	1M KOH	149	104	8
NiS ₂ nanosheets	1M NaOH	190	80	9
Ni ₃ S ₂ nanosheets	1M KOH	223	-	10
Ni ₃ S ₂ nanorods	1M KOH	200	107	11
NiS	1M KOH	380	-	12
NiS/Ni foam	1M KOH	158 (20 mA/cm ²)	83	13
NiCo ₂ S ₄ nanowires	1M KOH	228 (20 mA/cm ²)	141	14
Ni ₃ Se ₂ film	1M KOH	100	98	15
Pt/C	1M KOH	70	55	16
Co₉S₈-Ni_xS_y/Nif (500C 10m)	1M KOH	163	88	This work

Table S2 Comparison of the HER performance between selected electrocatalysts based on earth-abundant elements in alkaline media

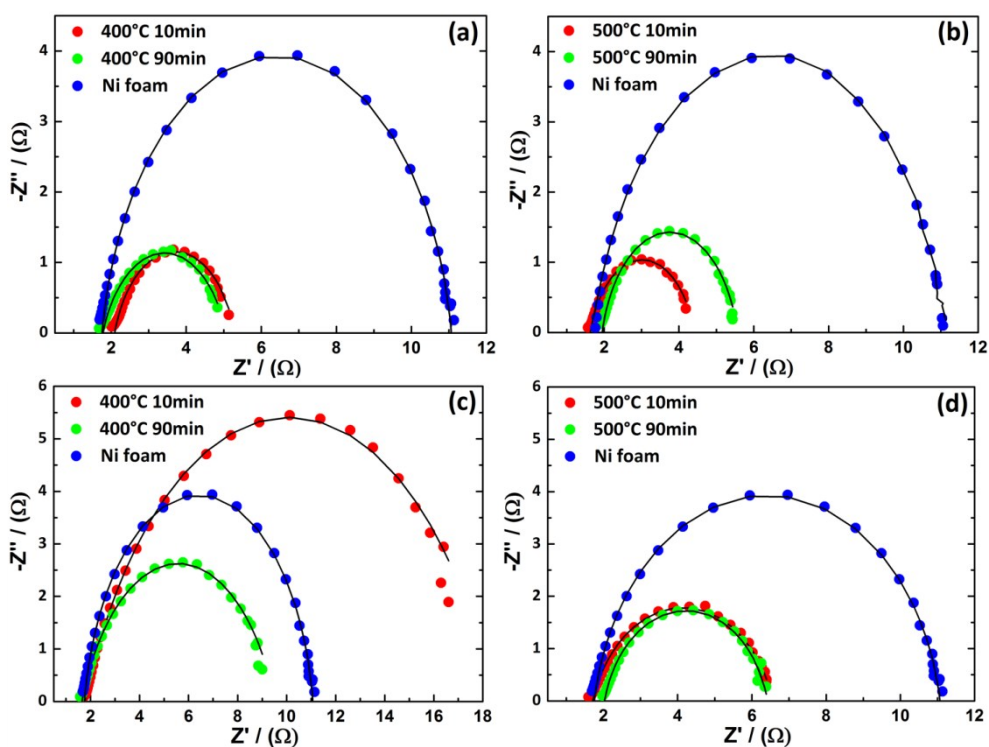


Fig. S12 Nyquist plots of (a)-(b) $\text{Co}_9\text{S}_8\text{-Ni}_x\text{S}_y/\text{NiF}$, (c)-(d) $\text{Ni}_3\text{S}_2/\text{NiF}$ recorded under potentiostatic mode at -0.230 V vs RHE in 1M KOH . The fitting was performed using the Randles circuit.

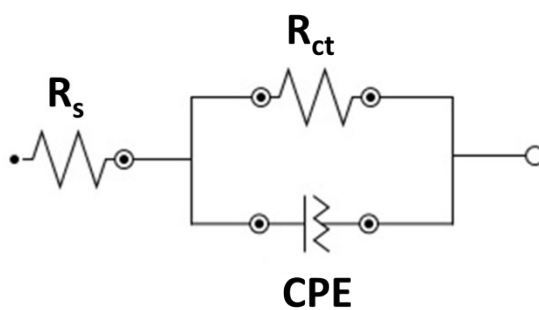


Fig. S13 Randles circuit used for the fitting of the EIS data; R_s , series resistance; R_{ct} , charge-transfer resistance; CPE, constant phase element

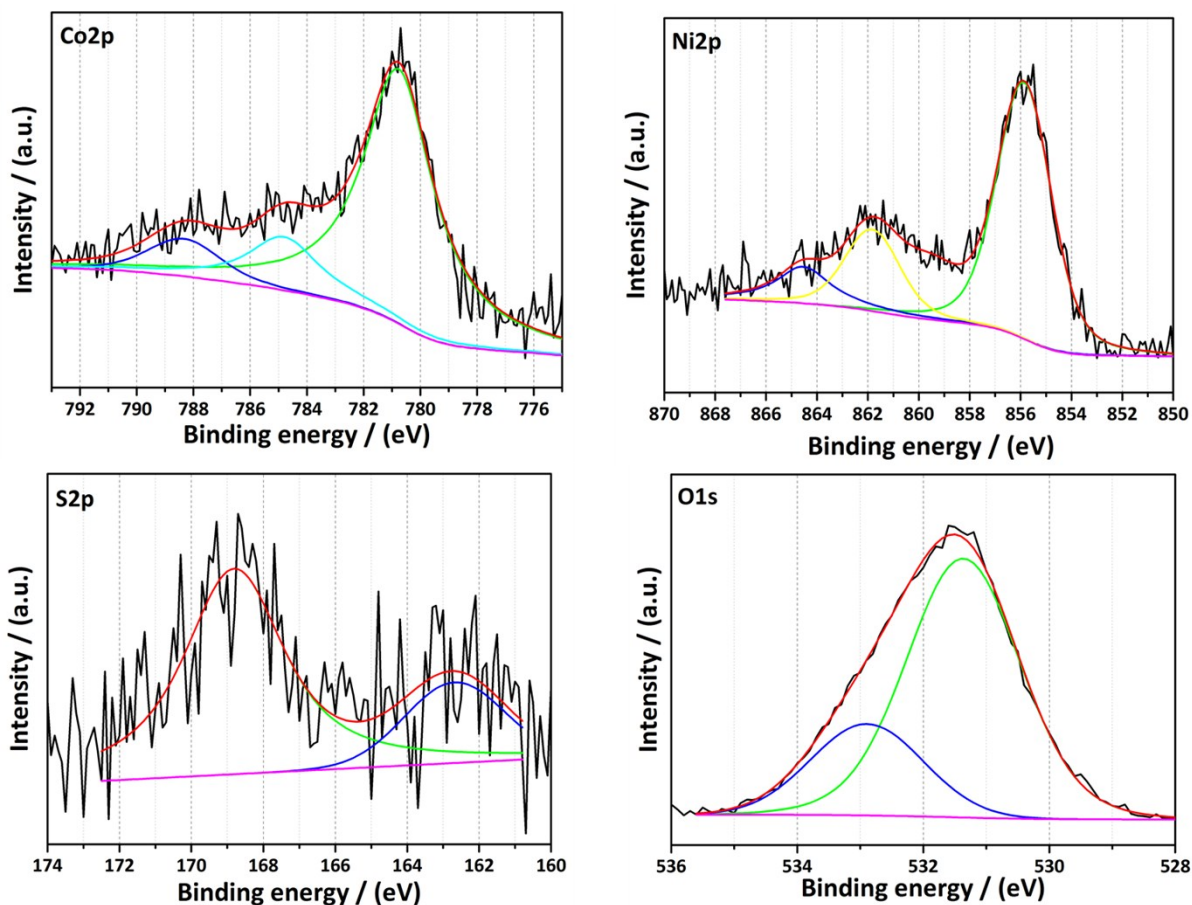


Fig. S14 XPS patterns for $\text{Co}_9\text{S}_8\text{-Ni}_x\text{S}_y/\text{Ni}$ annealed at 500°C 10 min after chronoamperometry test for 72 hours.

Annealing condition	Co/Ni atomic ratio	S/(Co+Ni) atomic ratio	$\text{Co}^{3+}/\text{Co}^{2+}$ atomic ratio	$\text{S}^{2-}/(\text{SO}_4^{2-})$ atomic ratio
500°C 10 min before chronoamperometry	0.53	0.74	0	1.32
500°C 10 min after chronoamperometry	1.15	0.81	0	0.31

Table S3 XPS quantitative analysis of the elemental composition on the surface of $\text{Co}_9\text{S}_8\text{-Ni}_x\text{S}_y/\text{Ni}$ electrode before and after the stability test.

References

- 1 N. Kumar, N. Raman and A. Sundaresan, *Zeitschrift für Anorg. und Allg. Chemie*, 2014, **640**, 1069–1074.
- 2 H. Zhang, Y. Li, G. Zhang, T. Xu, P. Wan and X. Sun, *J. Mater. Chem. A*, 2015, **3**, 6306–6310.
- 3 H. Zhang, Y. Li, G. Zhang, P. Wan, T. Xu, X. Wu and X. Sun, *Electrochim. Acta*, 2014, **148**, 170–174.
- 4 L.-L. Feng, M. Fan, Y. Wu, Y. Liu, G.-D. Li, H. Chen, W. Chen, D. Wang and X. Zou, *J. Mater. Chem. A*, 2016, -.
- 5 L. L. Feng, G. D. Li, Y. Liu, Y. Wu, H. Chen, Y. Wang, Y. C. Zou, D. Wang and X. Zou, *ACS Appl. Mater. Interfaces*, 2015, **7**, 980–988.
- 6 Y. Liang, Q. Liu, Y. Luo, X. Sun, Y. He and A. M. Asiri, *Electrochim. Acta*, 2016, **190**, 360–364.
- 7 T. Liu, Q. Liu, A. M. Asiri, Y. Luo and X. Sun, *Chem. Commun.*, 2015, **51**, 16683–6.
- 8 C. Tang, Z. Pu, Q. Liu, A. M. Asiri and X. Sun, *Electrochim. Acta*, 2015, **153**, 508–514.
- 9 X. Wu, B. Yang, Z. Li, L. Lei and X. Zhang, *RSC Adv.*, 2015, **5**, 32976–32982.
- 10 L. L. Feng, G. Yu, Y. Wu, G. D. Li, H. Li, Y. Sun, T. Asefa, W. Chen and X. Zou, *J. Am. Chem. Soc.*, 2015, **137**, 14023–14026.
- 11 C. Ouyang, X. Wang, C. Wang, X. Zhang, J. Wu, Z. Ma, S. Dou and S. Wang, *Electrochim. Acta*, 2015, **174**, 297–301.
- 12 D. Y. Chung, J. W. Han, D.-H. Lim, J.-H. Jo, S. J. Yoo, H. Lee and Y.-E. Sung, *Nanoscale*, 2015, **7**, 5157–5163.
- 13 W. Zhu, X. Yue, W. Zhang, S. Yu, Y. Zhang, J. Wang and J. Wang, *Chem. Commun.*, 2016, **1**, 3–6.
- 14 D. Liu, Q. Lu, Y. Luo, X. Sun and A. M. Asiri, *Nanoscale*, 2015, **7**, 15122–15126.
- 15 J. Shi, J. Hu, Y. Luo, X. Sun and A. M. Asiri, *Catal. Sci. Technol.*, 2015, **5**, 4954–4958.
- 16 L. Ma, L. R. L. Ting, V. Molinari, C. Giordano and B. S. Yeo, *J. Mater. Chem. A*, 2015, **3**, 8361–8368.